Competing Topological and Kondo Insulator Phases on a Honeycomb Lattice

Xiao-Yong Feng,[1,2] Jianhui Dai,[1,2,3] Chung-Hou Chung,[4,5] and Qimiao Si[6]

[1]*Condensed Matter Group, Department of Physics, Hangzhou Normal University, Hangzhou 310036, China*
[2]*Chen Jian Gong Institute for Advanced Study, Hangzhou Normal University, Hangzhou 310036, China*
[3]*Department of Physics, Zhejiang University, Hangzhou 310027, China*
[4]*Electrophysics Department, National Chiao-Tung University, HsinChu, Taiwan 300, Republic of China*
[5]*National Center for Theoretical Sciences, HsinChu, Taiwan 300, Republic of China*
[6]*Department of Physics and Astronomy, Rice University, Houston, Texas 77005, USA*

We investigate the competition between the spin-orbit interaction of itinerant electrons and their Kondo coupling with local moments densely distributed on the honeycomb lattice. We find that the model at half-filling displays a quantum phase transition between topological and Kondo insulators at a nonzero Kondo coupling. In the Kondo-screened case, tuning the electron concentration can lead to a new topological insulator phase. The results suggest that the heavy-fermion phase diagram contains a new regime with a competition among topological, Kondo-coherent and magnetic states, and that the regime may be especially relevant to Kondo lattice systems with $5d$-conduction electrons. Finally, we discuss the implications of our results in the context of the recent experiments on SmB_6 implicating the surface states of a topological insulator, as well as the existing experiments on the phase transitions in SmB_6 under pressure and in CeNiSn under chemical pressure.

Systems containing both itinerant electrons and local moments continue to attract intensive interest in modern condensed matter physics. The antiferromagnetic exchange coupling between the two components gives rise to the Kondo singlet ground state. Historically, the Kondo effect in a single local-moment impurity provided an understanding of the resistivity minimum in metals as well as the physics of dilute magnetic alloys and quantum nanostructures [1,2]. In the concentrated case, consideration of the Kondo effect and its competition with magnetically ordered ground states has been playing a central role in the understanding of the novel phases and quantum criticality of heavy fermion materials [3]. For the half-filled limit of the Kondo lattice system, the Kondo effect gives rise to the paramagnetic Kondo insulator (KI) state [2,4–6].

Recently, the quantum spin Hall insulator in two dimensions and the topological insulator (TI) more generally have attracted extensive interest [7,8]. These insulators have a charge excitation gap in the bulk, but support gapless surface states protected by time-reversal symmetry. The surface states constitute a helical liquid where the spin orientation is locked with the direction of electron momentum [9,10]. Although they are robust against weak disorders that preserve time-reversal symmetry, the surface states may be influenced by magnetic impurities. For example, the conductance of a one-dimensional edge helical liquid of a two-dimensional TI in the presence of a single magnetic impurity can exhibit a logarithmic behavior at high temperatures and goes to the unitarity limit at $T = 0$ due to the formation of a Kondo singlet [10,11]. This is in contrast to the Kondo problem in conventional Luttinger liquids, where even very weak Coulomb interaction leads to vanishing conductance at zero temperature [12]. Generally speaking, the Kondo screening of magnetic impurities on the surface of TIs may not necessarily be complete due to the $SU(2)$ breaking of the spin-orbit coupling (SOC) [13], and the effective Ruderman-Kittle-Kasuya-Yosida interaction between the local moments can be mediated by the edge carries, leading to an in-plane noncollinear and helical order [14–17]. For magnetic impurities in TIs, previous studies have focused on the effect of surface impurities, i.e., magnetic impurities positioned on the surface of TIs, or coupled effectively to the surface states [18]. Whether and how the bulk magnetic impurities influence the properties of TIs is largely an open problem.

From the perspective of heavy-fermion physics, very interesting properties are emerging from materials that involve $5d$ electrons, such as the pyrochlore $Pr_2Ir_2O_7$ [19]. The significant SOC of the $5d$ electrons may give rise to topologically nontrivial physics for the $5d$ electrons alone, raising the intriguing question of the interplay between topological and Kondo physics. The regime of transitions among the competing ground states represents a setting in which the effects of strong interactions on TIs may become more tractable. Furthermore, Kondo insulators themselves may become topological as a result of the symmetry properties of the hybridization matrix [20].

Motivated by these recent developments, in this letter we study a dense set of magnetic local moments interacting with the spin-orbit coupled itinerant electrons on the honeycomb lattice as illustrated in Fig. 1. Such a system is
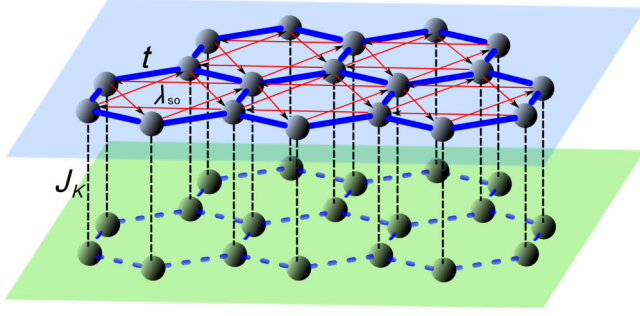
FIG. 1 (color online).   Itinerant electrons moving on a honey-comb lattice while coupled vertically to the local spins on a parallel lattice.

relevant for the graphene or magnetic moment interface and could be constructed through cold atoms in an optical lattice. The system could also be realized by growing a two-dimensional TI on an appropriate magnetic insulating substrate; similar heterostructures involving TI Bi_2Se_3 thin films and superconducting layers have already been fabricated by the molecular beam epitaxy technique [21]. It may very well be built based on the existing $5d$-electron-based iridates on the honeycomb lattice, such as Na_2IrO_3 [22]. Finally, given that recent experiments in SmB_6 have provided tentative evidence for the surface states of a topological insulator [23,24], our results here on the transitions between topological insulator and Kondo coherent states lead to the intriguing question of what happens to such surface states when SmB_6 and related intermetallic systems are tuned by external or chemical pressure (see below).

The model we consider, illustrated in Fig. 1, is specified by the Hamiltonian

$$H = -t \sum_{\langle \mathbf{ij} \rangle \sigma} c_{\mathbf{i}\sigma}^\dagger c_{\mathbf{j}\sigma} + i\lambda_{so} \sum_{\ll \mathbf{ij} \gg \sigma\sigma'} v_{\mathbf{ij}} c_{\mathbf{i}\sigma}^\dagger \sigma_{\sigma\sigma'}^z c_{\mathbf{j}\sigma'}$$
$$+ J_K \sum_{\mathbf{i}} \vec{s}_{\mathbf{i}} \cdot \vec{S}_{\mathbf{i}}, \qquad (1)$$

where $c_{\mathbf{i}\sigma}$ annihilates an electron at site $\mathbf{i}$ with spin component $\sigma = \uparrow, \downarrow$, $\vec{s}_{\mathbf{i}} = c_{\mathbf{i}\sigma}^\dagger(\vec{\sigma}_{\sigma\sigma'}/2)c_{\mathbf{i}\sigma'}$, and $\vec{S}_{\mathbf{i}}$ represents the local moments with $\vec{\sigma}$ being the Pauli matrices. The parameters t and λ_{so} are the nearest-neighbor hopping energy and the next-nearest-neighbor *intrinsic* (Dresselhaus-type) SOC of the conduction electrons, respectively, with $v_{\mathbf{ij}} = \pm 1$ depending on the direction of hopping between the next-nearest-neighbor sites. Finally, J_K is the antiferromagnetic Kondo coupling between the spins of conduction electrons and local impurities. The model Eq. (1) minimally interpolates the Kane-Mele Hamiltonian ($J_K = 0$) [9,25] and the standard Kondo lattice Hamiltonian ($\lambda_{so} = 0$). We note that recent studies have focused on the effect of Hubbard U interaction of the conduction electrons [26–31].

To proceed, we note that the model of Eq. (1) is connected to the Anderson lattice Hamiltonian,

$$H = H_{KM} + H_{cd} + H_d, \qquad (2)$$

where H_{KM} is the Kane-Mele Hamiltonian [the first two terms of Eq. (1)], $H_{cd} = V\sum_{\mathbf{i}\sigma}(c_{\mathbf{i}\sigma}^\dagger d_{\mathbf{i}\sigma} + \text{H.c.})$ is the hybridization between the itinerant electrons and localized d-electrons, and $H_d = E_0\sum_{\mathbf{i}\sigma} d_{\mathbf{i}\sigma}^\dagger d_{\mathbf{i}\sigma} + U\sum_{\mathbf{i}} n_{di\uparrow}n_{di\downarrow}$ is for the local electrons with E_0 being the local energy level and U the on-site Coulomb repulsion of local electrons. The models described by Eqs. (1) and (2) are equivalent provided that, in the absence of SOC, the d-electrons are in the Kondo regime (U is sufficiently large and E_0 is well below the Fermi energy (E_F) of the conduction band). In this regime, $J_K \sim V^2[(1/E_F - E_0) + (1/U - E_F + E_0)]$. Our calculations will be carried out in Eq. (2). As our focus is on the competition between the TI and KI at half-filling, we shall mainly consider the paramagnetic states.

In the momentum $\mathbf{k}$ space, the conduction electron part of the Hamiltonian takes the form of $H_{KM} = \sum_{\mathbf{k}\sigma} C_{\mathbf{k}\sigma}^\dagger M_{\mathbf{k}\sigma} C_{\mathbf{k}\sigma}$, with $C_{\mathbf{k}\sigma}^\dagger = (c_{a,\mathbf{k}\sigma}^\dagger, c_{b,\mathbf{k}\sigma}^\dagger)$ and

$$M_{\mathbf{k}\sigma} = \begin{pmatrix} \sigma\Lambda_{\mathbf{k}} - \mu & \epsilon_{\mathbf{k}} \\ \epsilon_{\mathbf{k}}^* & -\sigma\Lambda_{\mathbf{k}} - \mu \end{pmatrix}, \qquad (3)$$

where, $\sigma = +1$ and -1 refers to spin up and spin down, $\Lambda_{\mathbf{k}} = 2\lambda_{so}[\sin k_1 - \sin k_2 - \sin(k_1 - k_2)]$, $\epsilon_{\mathbf{k}} = -t(1 + e^{-ik_1} + e^{-ik_2})$. We have included the chemical potential μ term to control the electron filling. The subscripts a and b denote two sublattices of the honeycomb lattice as shown in Fig. 2. Each unit cell has two adjacent a, b sites, and the primitive vectors are $\mathbf{a}_1$ and $\mathbf{a}_2$.

For the local electrons, we consider the large-U limit and utilize the slave-boson method [1]. The local electrons are expressed as $d_{\mathbf{i}\sigma}^\dagger = f_{\mathbf{i}\sigma}^\dagger b_{\mathbf{i}}$, with $f_{\mathbf{i}\sigma}^\dagger$ and $b_{\mathbf{i}\sigma}$ being, respectively, fermionic and bosonic operators satisfying the constraint $b_{\mathbf{i}}^\dagger b_{\mathbf{i}} + \sum_\sigma f_{\mathbf{i}\sigma}^\dagger f_{\mathbf{i}\sigma} = 1$. Introducing the basis $\Psi_{\mathbf{k}\sigma}^\dagger = (c_{a,\mathbf{k}\sigma}^\dagger, c_{b,\mathbf{k}\sigma}^\dagger, f_{a,\mathbf{k}\sigma}^\dagger, f_{b,\mathbf{k}\sigma}^\dagger)$ in the $\mathbf{k}$ space, the mean-field Hamiltonian is expressed as $H_{MF} = \sum_{\mathbf{k}\sigma} \Psi_{\mathbf{k}\sigma}^\dagger H_{\mathbf{k}\sigma} \Psi_{\mathbf{k}\sigma}$ with

$$H_{\mathbf{k}\sigma} = \begin{pmatrix} M_{\mathbf{k}\sigma} & rVI \\ rVI & (E_0 + \lambda)I \end{pmatrix}. \qquad (4)$$

Here, I is a 2×2 identity matrix, $r = \langle b \rangle$ is the condensation density of the bosons, and λ is the Lagrange multiplier introduced to implement the constraint. We will carry out our calculations for $N = 2$ ($\sigma = \pm 1$); a large-N
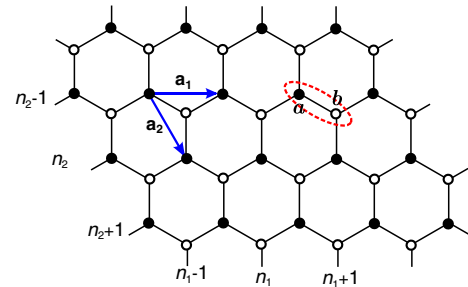

FIG. 2 (color online).   The unit cell and primitive translation vectors.

generalization in the presence of SOC may also be considered [32]. The quasiparticle bands of the mean-field Hamiltonian Eq. (4) are degenerate for the two spin components. For each spin component, the Hamiltonian can be diagonalized (even though the matrix is 4×4) giving rise to the quasiparticle dispersion

$$E_{\mathbf{k}}^{(1)} = \frac{1}{2}\left(G_{\mathbf{k}+} + \sqrt{G_{\mathbf{k}-}^2 + 4r^2V^2}\right) - \mu$$

$$E_{\mathbf{k}}^{(2)} = \frac{1}{2}\left(G_{\mathbf{k}-} + \sqrt{G_{\mathbf{k}+}^2 + 4r^2V^2}\right) - \mu$$

$$E_{\mathbf{k}}^{(3)} = \frac{1}{2}\left(G_{\mathbf{k}+} - \sqrt{G_{\mathbf{k}-}^2 + 4r^2V^2}\right) - \mu \qquad (5)$$

$$E_{\mathbf{k}}^{(4)} = \frac{1}{2}\left(G_{\mathbf{k}-} - \sqrt{G_{\mathbf{k}+}^2 + 4r^2V^2}\right) - \mu,$$

with $G_{\mathbf{k}\pm} = E_0 + \lambda + \mu \pm \sqrt{\Lambda_{\mathbf{k}}^2 + |\epsilon_{\mathbf{k}}|^2}$. The parameters r and λ are determined by the following equations:

$$\frac{1}{2\mathcal{N}} \sum_{\mathbf{k}\sigma;\alpha=a,b} \langle f_{\alpha,\mathbf{k}\sigma}^\dagger f_{\alpha,\mathbf{k}\sigma}\rangle + r^2 = 1 \qquad (6)$$

$$\frac{V}{2\mathcal{N}} \sum_{\mathbf{k}\sigma;\alpha=a,b} \Re\langle c_{\alpha,\mathbf{k}\sigma}^\dagger f_{\alpha,\mathbf{k}\sigma}\rangle + r\lambda = 0, \qquad (7)$$

with $\mathcal{N}$ being the total number of unit cells and $\Re$ indicating the real part. In the following we shall mainly consider the half-filled case, corresponding to $\mu = 0$.

The formation of the quasiparticle bands, specified by Eq. (5), requires the renormalized hybridization $V^* = rV \neq 0$. By contrast, if $V^* = 0$, the spectra separate into the decoupled conduction bands and local level. Moreover, the band inversion takes place at $V^* = 0$. While this feature is hidden and not important in ordinary Kondo lattice problems, it is crucial in the present problem because now the conduction bands are from the TI. As a consequence, the bulk gap of TI closes at the onset of V^*, leading to a quantum phase transition to the KI.

At zero temperature, r (or V^*) is nonzero only if V is larger than a critical V_c, as a result of the suppressed density of conduction electron states for a honeycomb lattice. Figure 3(a) shows the numerical results for the V dependence of r for several values of λ_{so}. The local level E_0 is taken at the bottom of the conduction band. The critical $V_c \sim 1.3$ for $\lambda_{\mathrm{so}} = 0$, and increases almost linearly with λ_{so}, as seen in the inset of Fig. 3(a). When $V < V_c$, $r = 0$, indicating the Kondo destruction, so the system remains in the TI phase with a bulk gap $\Delta_T = 6\sqrt{3}\lambda_{so}$. While for $V > V_c$, $r \neq 0$, the Kondo screening emerges and the band inversion takes place immediately, so the system enters into the KI phase. For small r, the KI phase has a finite hybridization gap $\Delta_K \sim 2r^2V^2/3t$. This is the direct band gap at the Γ-point where the contribution from the SOC vanishes.

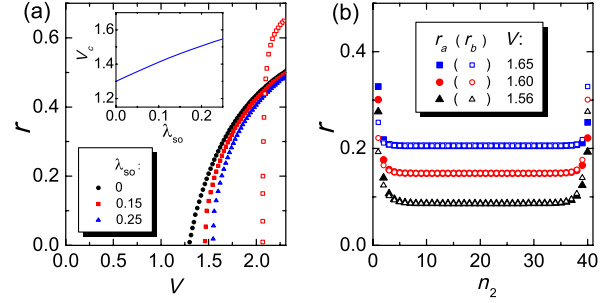It is interesting to compare the results here for the Kondo-lattice problem with those for its counterpart of a

FIG. 3 (color online).　(a) Large system with periodic boundary condition: The mean-field parameter r as a function of V for $\lambda_{\mathrm{so}} = 0$, 0.15, and 0.25. As a comparison, the red open square is for the corresponding single-ion Kondo problem for $\lambda_{\mathrm{so}} = 0.15$. The inset shows the critical V_c as a function of λ_{so}. All the coupling constants are in unit of t. (b) The site dependence of r for the lattice with zig-zag edges for several V in the Kondo phase, the width $N_2 = 40$, $\lambda_{\mathrm{so}} = 0.15$.

single ion magnetic impurity imbedded in the bulk of the two-dimensional TI. Using the same method, and for $\lambda_{\mathrm{so}} = 0.15$ as an example shown in Fig. 3(a), we find $V_c \sim 2.07$ for the single ion Kondo screening which is much larger than $V_c \sim 1.45$ determined here. In the absence of SOC, the finite V_c is due to the fact that the electron host is a pseudogap system so that the single ion Kondo screening needs a nonzero Kondo coupling comparable to the gap amplitude [33–35]. The enhancement of Kondo effect comparing to the single ion Kondo screening is similar to the Kondo lattice with d-wave superconducting conduction electrons [36].

We next investigate the surface states of the finite system with boundaries. We take a two-dimensional ribbon by cutting two zig-zag edges with width N_2, while the size along $\mathbf{a}_1$ remains infinite. Then the boson mean-field r is dependent on the coordinate n_2 and the sublattices and can be denoted by $r_a(n_2)$ and $r_b(n_2)$, respectively. We have $r_b(n_2) = r_a(N_2 - n_2)$ due to the inversion symmetry. Figure 3(b) shows the site dependence of r_a and r_b for $N_2 = 40$ and $\lambda_{\mathrm{so}} = 0.15$. A general feature is that r decreases rapidly from the edge to the bulk. This feature is attributed to the gapless edge states. $r(n_2)$ is almost flat away from the edges ($5 < n_2 < 35$) as shown in Fig. 3(b), indicating that the finite size effect is relatively small for $N_2 = 40$.

Figure 4 shows the energy spectra with four sets of parameters; here, $\mu = 0$ is imposed. Figures 4(a) and 4(b) display the spectra of the conduction electrons in the absence of the Kondo singlet ($V^* = 0$) and for $\lambda_{\mathrm{so}} = 0$, 0.03, respectively. The edge states with a single Dirac point at the Fermi energy in Fig. 4(b) manifest the TI phase [9,25]. In comparison, Figs. 4(c) and 4(d) are the spectra for $V > V_c$. The Kondo-singlet formation is clearly reflected in the hybridization gap at half filling and the relatively narrow flat bands near the Fermi energy (near the transition point the flatness is measured by t/V^*).

Furthermore, we observe that in the KI phase, the narrow bands can be separated from the continuum by
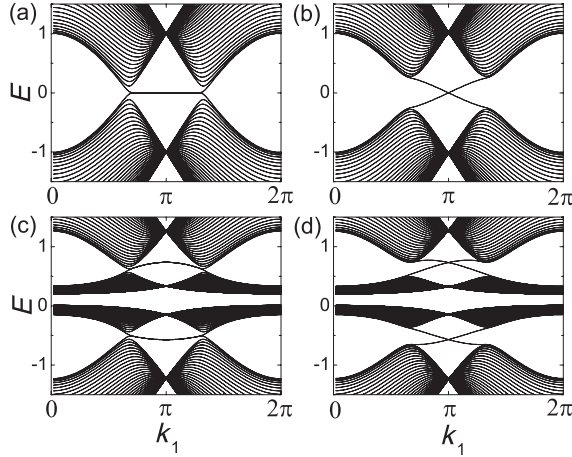
FIG. 4. The energy spectra for a ribbon of width $N_2 = 40$.
(a) $V = 0$ and $\lambda_{so} = 0$; (b) $V = 0$ and $\lambda_{so} = 0.03$; (c) $V = 1.7$
and $\lambda_{so} = 0$; (d) $V = 1.7$ and $\lambda_{so} = 0.03$.

increasing the SOC, leading to a bulk gap at the 1/4 or 3/4
fillings (achieved by tuning the chemical potential $\mu \neq 0$).
This is the direct band gap between $E_{\mathbf{k}}^{(3)}$ and $E_{\mathbf{k}}^{(4)}$ or between
$E_{\mathbf{k}}^{(1)}$ and $E_{\mathbf{k}}^{(2)}$ at the points $(2\pi/3, 4\pi/3)$ and $(4\pi/3, 2\pi/3)$,
respectively, with the gap magnitude $\Delta_{KT} \sim 6\sqrt{3}r^2 V^2 \lambda_{so}/\mu^2$
for the large bulk system. Moreover, for the finite system with
boundaries, the edge states emerge again with a Dirac point
within the bulk gap. This feature is robust for a range of the
chemical potential μ corresponding to the 1/4 or 3/4 filling.
We have also calculated the $\mathbb{Z}_2$ topological bulk invariant
Ξ_{2D} following the monodromy approach developed in
Ref. [37]. The result confirms that $\Xi_{2D} = 1$ at half filling
and $\Xi_{2D} = -1$ at 1/4 or 3/4 filling. Therefore, the insulat-
ing phase at 1/4- or 3/4-filling is topologically nontrivial,
and its surface states, while having the spin direction locked
by the momentum, contain the contributions from both
conduction and local electrons. Hence in the case of
Fig. 4(d) we have a new TI phase with the Kondo-singlet
formation and a surface heavy-fermion helical liquid.

We now consider the TI-KI transition around V_c. In the
present analysis at the saddle-point level, the onset of
Kondo effect is continuous [Fig. 3(a)]. Correspondingly,
the KI gap sets in continuously. By contrast, on the TI side
there is simply a decoupling of the conduction-electron and
local-moment components. However, we show that the
quantum fluctuations beyond the saddle point reduce the
bulk gap from the TI side, as is described in some detail in
the Supplemental Material [38]. The situation is similar to
the case of single-impurity pseudogapped Kondo problem,
for which numerical renormalization group calculations,
for instance, establish a well-defined second-order phase
transition for the Kondo-destruction quantum critical point
[39]. In the lattice case, the Ruderman-Kittle-Kasuya-
Yosida interaction between the local moments, which is
mediated by Kondo coupling in our model, will also induce
magnetic order. Taking into account the magnetic order
will leave the KI phase intact; as is standard, the Kondo

screening present in the KI phase quenches the local
moments and their ordering tendency. In the TI phase,
we have explicitly shown (in the SM) that an antiferro-
magnetic order, characterized by the order parameter M,
will reduce the TI bulk gap to $\Delta_T = 2(3\sqrt{3}\lambda_{so} - J_K M)(1 - V^2/E_0^2)$. This TI gap remains nonzero for a
finite range of M and V; in other words, the TI phase
remains stable in the presence of an antiferromagnetic
order for a range of $V < V_c$. Our results can be understood
based on general arguments: in the presence of magnetic
order, the Z_2 topological invariant is replaced by two spin-
Chern numbers which remain unchanged when the time
reversal symmetry is broken by the magnetic order [40,41].
Meanwhile, the surface states remain gapless unless the
bulk gap closes [42,43].

While detailed transitions among KI and TI phases, on the
one hand, and antiferromagnetic order on the other is be-
yond the scope of the present work, our work does reveal
that the heavy-fermion phase diagram contains a hitherto
unexplored new regime with a competition among topologi-
cal, Kondo-coherent, and magnetic states; such competition
involves the physics of Kondo destruction and associated
local quantum criticality [44]. In other words, when the
magnetic order and related dynamical effects are incorpo-
rated in our analysis, the TI-KI transition discussed here will
represent a regime where topological effects strongly inter-
play with the onset of magnetism and Kondo coherence. The
simplification that proximity to quantum criticality brings
may very well make the interaction effects on the TI phase
and its associated surface states more tractable.

We close by noting that we have treated the hybridization
to be $\mathbf{k}$ independent. When the spin and $\mathbf{k}$ dependences of
the hybridization are incorporated, part of the KI phase may
itself become topological, as emphasized in Ref. [20].

We now briefly discuss our work in the context of $4f$-
electron-based Kondo insulators. In SmB_6, it is known that a
sufficiently large external pressure collapses the Kondo
coherence in SmB_6 and turns it into an antiferromagnetic
metallic state [45]. Combined with the recent experimental
evidence in SmB_6 for the edge states of a topological
insulator [23,24], this is reminiscent of the transition among
the topological and Kondo-coherent or magnetic states
implicated by the present study. An intriguing question
then arises, which deserves the study of future experiments:
what happens to the candidate chiral edge states when SmB_6
is placed under external pressure? Along a similar line,
CeNiSn is another intermetallic system believed to be a
Kondo insulator. In CeNiSn, (negative) chemical pressure
achieved through Pd or Pt substitution for Ni is known to
induce a transition out of its Kondo insulator state [46–49].
It will therefore be informative to explore surface states in
the $Ce(Pt_{1-x}Ni_x)Sn$ and $Ce(Pd_{1-x}Ni_x)Sn$ series. Finally, it
is worth noting that CePtSn has the distinction of involving
$5d$ electrons with a large SOC.

To summarize, we have considered the effect of SOC of
the conduction electrons in a Kondo-lattice system. Our

study offers the first qualitative understanding of the competition between topological and Kondo insulator ground states on a simple and yet generic model in two dimensions. While our analysis has so far been primarily confined to the paramagnetic cases, our results already suggest that the overall phase diagram of heavy-fermion systems includes a new regime with competition among topological, Kondo-coherent, and magnetic states. This regime should be particularly prominent for heavy fermion systems whose conduction electron band is associated with the strongly spin-orbit-coupled $5d$ electrons. As such, our work opens up a new regime of physical interest for compounds based on iridium, platinum, and related $5d$ elements.

[1] A. C. Hewson, *The Kondo Problem to Heavy Fermions* (Cambridge University Press, Cambridge, England, 1993).
[2] P. Coleman, in *Handbook of Magnetism and Advanced Magnetic Materials* (Wiley, New York, 2007), Vol. 1, p. 95.
[3] P. Gegenwart, Q. Si, and F. Steglich, Nat. Phys. **4**, 186 (2008).
[4] G. Aeppli and Z. Fisk, Comments Cond. Mat. Phys. **16**, 155 (1992).
[5] H. Tsunetsugu, M. Sigrist, and K. Ueda, Rev. Mod. Phys. **69**, 809 (1997).
[6] P. Riseborough, Adv. Phys. **49**, 257 (2000).
[7] M. Z. Hasan and C. L. Kane, Rev. Mod. Phys. **82**, 3045 (2010).
[8] X.-L. Qi and S.-C. Zhang, Rev. Mod. Phys. **83**, 1057 (2011).
[9] C. L. Kane and E. J. Mele, Phys. Rev. Lett. **95**, 226801 (2005).
[10] C. Wu, B. A. Bernevig, and S.-C. Zhang, Phys. Rev. Lett. **96**, 106401 (2006).
[11] J. Maciejko, C. Liu, Y. Oreg, X.-L. Qi, C. Wu, and S.-C. Zhang, Phys. Rev. Lett. **102**, 256803 (2009).
[12] C. L. Kane and M. P. A. Fisher, Phys. Rev. B **46**, 15233 (1992).
[13] X.-Y. Feng, W.-Q. Chen, J.-H. Gao, and F.-C. Zhang, Phys. Rev. B **81**, 235411 (2010).
[14] J. Gao, W. Chen, X. C. Xie, and F.-C. Zhang, Phys. Rev. B **80**, 241302 (2009).
[15] R. R. Biswas and A. V. Balatsky, Phys. Rev. B **81**, 233405 (2010).
[16] I. Garate and M. Franz, Phys. Rev. Lett. **104**, 146802 (2010).
[17] J. J. Zhu, D. X. Yao, S. C. Zhang, and K. Chang, Phys. Rev. Lett. **106**, 097201 (2011).
[18] See also, e.g., J. Maciejko, Phys. Rev. B **85**, 245108 (2012).
[19] S. Nakatsuji, Y. Machida, Y. Maeno, T. Tayama, T. Sakakibara, J. Duijn, L. Balicas, J. Millican, R. Macaluso, and J. Chan, Phys. Rev. Lett. **96**, 087204 (2006).
[20] M. Dzero, K. Sun, V. Galitski, and P. Coleman, Phys. Rev. Lett. **104**, 106408 (2010).
[21] M. X. Wang et al., Science **336**, 52 (2012).
[22] Y. Singh, S. Manni, J. Reuther, T. Berlijn, R. Thomale, W. Ku, S. Trebst, and P. Gegenwart, Phys. Rev. Lett. **108**, 127203 (2012); Y. Singh and P. Gegenwart, Phys. Rev. B **82**, 064412 (2010).
[23] S. Wolgast et al., arXiv:1211.5104.
[24] J. Botimer et al., arXiv:1211.6769.
[25] C. L. Kane and E. J. Mele, Phys. Rev. Lett. **95**, 146802 (2005).
[26] S. Rachel and K. Le Hur, Phys. Rev. B **82**, 075106 (2010).
[27] M. Hohenadler, T. C. Lang, and F. F. Assaad, Phys. Rev. Lett. **106**, 100403 (2011).
[28] S.-L. Yu, X. C. Xie, and J.-X. Li, Phys. Rev. Lett. **107**, 010401 (2011).
[29] D.-H. Lee, Phys. Rev. Lett. **107**, 166806 (2011).
[30] D. Zheng, G.-M. Zhang, and C. Wu, Phys. Rev. B **84**, 205121 (2011).
[31] J. Quan et al., arXiv:1201.1698.
[32] M. Dzero, Eur. Phys. J. B **85**, 297 (2012).
[33] D. Withoff and E. Fradkin, Phys. Rev. Lett. **64**, 1835 (1990).
[34] K. Ingersent, Phys. Rev. B **54**, 11936 (1996).
[35] B. Uchoa, T. G. Rappoport, and A. H. Castro Neto, Phys. Rev. Lett. **106**, 016801 (2011).
[36] D. E. Sheehy and J. Schmalian, Phys. Rev. B **77**, 125129 (2008).
[37] E. Prodan, Phys. Rev. B **83**, 235115 (2011).
[38] See Supplemental Material at http://link.aps.org/supplemental/10.1103/PhysRevLett.111.016402 for discussions on the effects of quantum fluctuations of the slave bosons and magnetic order of the local moments.
[39] K. Ingersent and Q. Si, Phys. Rev. Lett. **89**, 076403 (2002).
[40] D. N. Sheng, Z. Y. Weng, L. Sheng, and F. D. M. Haldane, Phys. Rev. Lett. **97**, 036808 (2006).
[41] E. Prodan, Phys. Rev. B **80**, 125327 (2009).
[42] Y. Yang, Z. Xu, L. Sheng, B. Wang, D. Y. Xing, and D. N. Sheng, Phys. Rev. Lett. **107**, 066602 (2011).
[43] H. Li, L. Sheng, and D. Y. Xing, Phys. Rev. Lett. **108**, 196806 (2012).
[44] S. J. Yamamoto and Q. Si, J. Low Temp. Phys. **161**, 233 (2010).
[45] A. Barla, J. Derr, J. P. Sanchez, B. Salce, G. Lapertot, B. P. Doyle, R. Rüffer, R. Lengsdorf, M. M. Abd-Elmeguid, and J. Flouquet, Phys. Rev. Lett. **94**, 166401 (2005).
[46] J. Sakurai, R. Kawamura, T. Taniguchi, S. Nishigori, S. Ikeda, H. Goshima, T. Suzuki, and T. Fujita, J. Magn. Magn. Mater. **104–107**, 1415 (1992).
[47] D. T. Adroja, B. D. Rainford, A. J. Neville, and A. G. M. Jansen, Physica (Amsterdam) **223B–224B**, 275 (1996).
[48] G. M. Kalvius, A. Kratzer, G. Grosse, D. R. Noakes, R. Wäppling, H. v. Löhneysen, T. Takabatake, and Y. Echizen, Physica (Amsterdam) **289B–290B**, 256 (2000).
[49] M. Kasaya, T. Tani, H. Suzuki, K. Ohoyama, and M. Kohgi, J. Phys. Soc. Jpn. **60**, 2542 (1991).